Translational symmetry breaking in holographic strange metals

Balm, F.A.

3. Numerical Holography and Lattices

The effort of breaking translational symmetry inhomogeneously in holographic condensed matter systems goes back over a decade. The basic idea rather simple. Translational symmetry breaking is introduced explicitly by modulating one of the source terms of the field theory. There are different setups with different fields being sourced, and there are many things that can be computed, but first let us focus on the generics, how the translational symmetry is broken and what the general improvements in the works related to this thesis have been to various existing setups in order to get more accurate results. [107, 111, 114, 118–124]

Now let us finally break the translational symmetry, but keep the setup static, without any time dependence. While we can in principle use holography to compute non-stationary, time-dependent black holes, this is technically extremely challenging, not to mention in the presence of translational symmetry breaking.[125] As mentioned before, the static solution is thought to describe late-time locally thermally equilibrated states.

3.1. Spatial Modulation

The first real calculations using holographic lattices were done by Horowitz, Santos and Tong, where they took Reissner-Nordström and imposed a lattice in two different ways, first by modulating the the source term of an extra backreacted scalar field, and also by modulating the chemical potential.[118, 120] The modulation of the chemical potential is what comes closest to reproducing an actual 'ionic lattice', where regions of high and low chemical potential are spatially distributed, and have regions of low and high charge density associated with them, without the need for extra scalar fields.

The procedure to do this increases in complexity the more dimensions get their translational symmetry broken. I will first state the most general ansatz that is used for two-dimensional lattices. After this, I will show an example computation for a one-dimensional lattice in RN without extra scalars, as this simplifies the setup considerably and allows for the highlighting of some important points.

3.1.1. Bidirectional Lattices

The lattices presented in this thesis have translational symmetry broken in either one or two directions in the boundary. The mechanism by which this was imposed is general in both RN and GR black holes. It is possible to have a wide variety of extra phenomena take place, for example pseudoscalars that spontaneously break translational symmetry.[119, 121, 126] However, research

projects started in these directions were never brought to a satisfying conclusion, and are therefore not included in this thesis. In this work, only the chemical potential, set by $A_t(z=0)$, is modulated explicitly.

3.1.2. RN Lattice Model

The action and equations of motion for the full Reissner-Nordström setup are given by

$$S = \int d^4x\sqrt{-g}\left(R - 2\Lambda - \frac{1}{4}F_{\mu\nu}F^{\mu\nu}\right). \tag{3.1}$$

with associated Einstein and Maxwell equations

$$\begin{aligned} R_{\mu\nu} + 3g_{\mu\nu} &= \frac{1}{2}\left(F_{\mu\rho}F_{\nu}{}^{\rho} - \frac{1}{4}g_{\mu\nu}F_{\rho\sigma}F^{\rho\sigma}\right), \\ \nabla_\mu F^{\mu\nu} &= 0. \end{aligned} \tag{3.2}$$

Since time-reversal symmetry is not broken, it is possible to find solutions to the equations of motion where 8 fields are coupled together: the time component of the gauge field, the diagonal metric terms, and the spatial-radial off-diagonal metric terms. Other terms, such as the spatial terms of the gauge field, do not couple in as these would present themselves as effective magnetic fields in the electromagnetic field strength tensor. We do not break time reversal symmetry in our lattice, which means that these modes decouple. There is still some gauge freedom stemming from diffeomorphism invariance, which expresses itself in the Einstein equations by yielding constraint equations rather than dynamical equations for some of its components. These gauge freedoms will need to be fixed, more on which will follow in section 3.1.3. In general then we need to therefore solve for all 8 fields non-linearly simultaneously in order to obtain a fully back-reacted solution.

The metric is most conveniently parameterized via

$$\begin{aligned} ds^2 &= \frac{1}{z^2}\left(-Q_{tt}f(z)\eta_t^2 + Q_{xx}\eta_x^2 + Q_{yy}\eta_y^2 + \frac{1}{f(z)}Q_{zz}dz^2\right), \\ \eta_t &= dt, \\ \eta_x &= dx + Q_{xy}dy + Q_{xz}dz, \\ \eta_y &= dy + Q_{yz}dz, \end{aligned} \tag{3.3}$$

accompanied by the gauge field

$$A = \bar{\mu}(1-z)a_t dt \tag{3.4}$$

.

The function $f(z)$ is kept fixed here to be equal to that in equation (2.32)

$$f(z) = (1-z)\left(1 + z + z^2 - \frac{\mu^2 z^3}{4}\right). \tag{3.5}$$

In principle, these functions Q_{ij}, a_μ, φ can be functions of x, y and z, where we do not allow time dependence in order to maintain the static black hole. Translational symmetry breaking is wired in as follows. We will always restrict to rectangular lattice setups[1], where we assume that there are two independent periodicities going on in both of the transverse directions where we identify the coordinates

$$x \sim x + L_x, \quad y \sim y + L_y. \tag{3.6}$$

All of the functions Q_{ij}, a_μ, φ will therefore be assumed to have the same periodicity. For purely spontaneous translational symmetry breaking considerations this is all that is done, although one must be careful to pick a period which is compatible with the preferred wave vector of the instability. In the case of explicit modulation we choose the chemical potential to be also some periodic function with the same period, however we can choose freely how to fill this in. In practice, we always use a single harmonic potential in one or two directions to fill the periodic domain, but it is possible to have multiple periods of the explicit potential in the domain. This means that the time component of the gauge field can go like

$$a_t(x, y, z = 0) = \bar{\mu}\left(1 + \mathcal{A}_x \cos\left(G_x x\right) + \mathcal{A}_y \cos\left(G_y y\right)\right). \tag{3.7}$$

In order to satisfy periodic boundary conditions, this must mean that

$$L_{x,y} = \frac{2\pi N_{x,y}}{G_{x,y}}. \tag{3.8}$$

The resulting Einstein equations, when the ansatz is plugged in, is to not mince words a complete mess. There are many hundreds or thousands of terms following from all the different combinations of derivatives and non-linearities.[2] In the presence of any kind of translational symmetry breaking there is no analytical non-perturbative solution, and therefore the equations of motion (3.2) have to be evaluated numerically. In order to properly numerically evaluate this problem, we want to be able to phrase this as a boundary value problem. Two of the boundaries, namely in the x and y directions are straightforward, as periodic boundary conditions will impose conditions on the fields and their derivatives at the points of identification over the entire range of z. The boundary conditions on both ends of the radial direction require a bit more thought. At the boundary we want to impose AdS asymptotics —we are doing AdS/CFT after all —possibly supplemented by our explicit translational symmetry breaking term. At the horizon it is regularity of the fields, as well as the requirement of constant temperature across the black hole horizon that yields enough boundary conditions for a well-posed boundary value problem.

To give a quick summary, at the boundary we can impose that only the diagonal metric fields are equal to 1, which recovers AdS asymptotics

$$Q_{ij,i=j}\big|_{z=0} = 1, \quad Q_{ij,i\neq j}\big|_{z=0} = 0. \tag{3.9}$$

[1] Note that the ansatz presented above is slightly less general than the one presented in [127], but is much more straightforward to deal with in the case of rectangular lattices. The reduced complexity of the ansatz also makes it easier for computer algebra software to handle the very large equations that come out when the equations of motion are applied to this ansatz.

[2] Anecdotally, these equations can become so big that when compiled into C-code, simply cannot handle the sheer size and errors out.

along with a gauge field

$$\bar{\mu} a_t\big|_{z=0} = \mu(x, y) \tag{3.10}$$

The chemical potential $\mu(x, y)$ is what can set our explicit ionic lattice, via

$$\mu(x, y) = \bar{\mu}\, a_t(x, y) = \bar{\mu} \left(1 + \mathcal{A}_x \cos(G_x x) + \mathcal{A}_y \cos\big(G_y y\big)\right). \tag{3.11}$$

The boundary conditions at the horizon at $z = 1$ follow from regularity and can be found imposing a series expansion on the equation of motion after gauge fixing[3] in powers of $z - 1$ and requiring that each of the terms in the series expansions vanish. This will give a set of in general non-linear boundary equations of the form

$$\partial_z F_i\big|_{z=1} = g\left(\{F_j, \partial_x F_j, \partial_y F_j\}\right), \tag{3.12}$$

or in other words, boundary conditions can be found for the radial derivatives of all the fields F in the ansatz in terms of all the other fields and their tangential derivatives on the horizon. This is then supplemented by the condition

$$Q_{tt}\big|_{z=1} = Q_{zz}\big|_{z=1} \tag{3.13}$$

which encodes for the surface gravity and therefore temperature to be constant across the black hole horizon.

3.1.3. DeTurck Method

There is one major thing missing from the equations before they can be solved. The Einstein equations are hyperbolic-elliptical, which poses problems for any numerical effort.[128, 129] The problem that has been posed throughout section 3.1 so far ostensibly has the form of a boundary value problem. This type of problem, especially in a non-linear setting, lends itself very well to numerical approaches when the problem is elliptic. This is due to the fact that the eigenvalues of the principal symbol of an elliptic problem all have the same sign, and therefore it is possible to use relaxation-like approaches, where we start from an initial guess and let the system 'settle' into the true solution. The Einstein equations as we posed them are not elliptic.[128] Instead, due to gauge freedom, it is only elliptic for the physical degrees of freedom. The way this problem is phrased leaves some room for gauge freedom, which presents itself as an invariance under coordinate reparametrization. The exact phrasing and solution to this problem have been described in great detail.[129] The main message to take away is that we want to fix this gauge invariance in our equations, which would render the equations for all fields elliptic. This is one by using the DeTurck method, also known as the DeTurck trick.[130] The equation of motion for the gauge field in the explicit lattice does not require a gauge fix, as typically radial gauge $a_z = 0$ is chosen.

The problem is in essence that we can decompose any perturbation to a solution to the equations of motion into a pure gauge and a transverse part. The principal symbol acting on the pure gauge mode actually annihilates it. This makes the equations for the gauge degrees of freedom into some

[3] See sections 3.1.3.

kind of lower-order constraint equations in this system. The fix comes by picking a particular vector ξ^μ, the DeTurck vector, which is defined by

$$\xi^\lambda = g^{\mu\nu}\left(\Gamma^\lambda_{\mu\nu} - \bar{\Gamma}^\lambda_{\mu\nu}\right). \tag{3.14}$$

Here $\bar{\Gamma}^\lambda_{\mu\nu}$ is the Christoffel symbol for some reference metric, which is a known solution to the Einstein equations. Choosing a gauge then can be done by for example choosing $\xi^\mu = 0$. This is still a constraint equation. However, we can be even smarter about this, and generate what is called the Harmonic Einstein equations. First we define the harmonic Ricci tensor as

$$R^H_{\mu\nu} = R_{\mu\nu} - \nabla_{(\mu}\xi_{\nu)}, \tag{3.15}$$

which we insert into the equations of motion by simply taking $R_{\mu\nu} \to R^H_{\mu\nu}$. This turns the set of equations into a manifestly elliptic one. It turns out that finding a solution to the harmonicized equations of motion will then simultaneously take care of solving the original equations of motion as well as the gauge condition. Additionally, finding a solution and showing that its DeTurck vector vanishes guarantees that the solution is not a Ricci soliton.[128]

3.1.4. Thermodynamics of the Lattices

Assuming that a solution to the equations of motion has been found, the first thing that is possible to do is to evaluate the thermodynamics of the phase. The procedure is essentially the same as outlined in section 2.5. The difference now is that the components of the metric and gauge field are now not analytically known, but instead we have to work with numerical values and their numerical derivatives. We can perform a near-boundary expansion up to order z^3, and use the equations of motion to constrain several of the terms that appear in the boundary expansion. Using the expansions we can find the expressions that are summarized in table 3.1. The field theory

$$\begin{aligned}
\langle T^t_t\rangle/\bar{\mu}^3 &= \left(-2 - \tfrac{\bar{\mu}^2}{2} + \tfrac{1}{2}\partial_z^3 Q_{tt}\right)\Big|_{z=0}, \\
\langle T^x_x\rangle/\bar{\mu}^3 &= \left(1 + \tfrac{\bar{\mu}^2}{4} + \tfrac{1}{2}\partial_z^3 Q_{xx}\right)\Big|_{z=0}, \\
\langle T^y_y\rangle/\bar{\mu}^3 &= \left(1 + \tfrac{\bar{\mu}^2}{4} + \tfrac{1}{2}\partial_z^3 Q_{yy}\right)\Big|_{z=0}, \\
\rho/\bar{\mu}^2 &= \left(a_t - \partial_z a_t\right)/\bar{\mu}\Big|_{z=0}, \\
\mu/\bar{\mu} &= a_t\Big|_{z=0}, \\
S/\bar{\mu}^2 &= 4\pi\sqrt{Q_{xx}Q_{yy}}/\bar{\mu}^2\Big|_{z=1}.
\end{aligned}$$

Table 3.1.: Observables in the RN Lattice in terms of the UV expansions of the fields in the ansatz, where values per unit cell can be obtained by averaging over the unit cell in the transverse directions.

is still conformal, provided one uses the correct prescription in GR models explained in chapter 5, as the trace of the stress tensor still vanishes:

$$\left\langle T_t^t + T_x^x + T_y^y \right\rangle \propto \left(\partial_z^3 Q_{tt} + \partial_z^3 Q_{xx} + \partial_z^3 Q_{yy} \right) \Big|_{z=0} = 0, \tag{3.16}$$

which can be found as a constraint for the third-order components from the near-boundary expansion of the equations of motion. The accuracy to which this holds can be used as a convergence check, since a well-converged solution will have equation (3.16) vanish to some good accuracy.

3.2. Solutions to the Unidirectional Lattice

Numerical solutions to this differential equation problem need to deal with another problem: the equations are not well defined at the horizon and boundary, as some coefficients of the equations scale as z^{-4} as $z \to 0$. Therefore, simply putting it in a black-box algorithm like Mathematica's `NDSolve` is unlikely to provide useful results, as it will attempt to evaluate the equations of motion so close to the boundary that this results in an incredibly stiff problem. One option is to make an explicit series expansion to some finite cut-off and integrating from there.[131] This method was used in many early constructions of numerical holography, and can be improved by going either to a high order in series expansion or making the cut-off very small. This has some disadvantages, as explicitly constructing the power expansion required to get high accuracy becomes quite cumbersome especially when the boundary starts to have one or two transverse spatial dimensions. Due to the nature of the Einstein equations these are simply big expansions, and take a long time to compute even with modern computer algebra systems.

The alternative is to discretise the problem on a structured grid, where there is one set of grid points located at the boundary, and another some finite δz away from it. On this grid, we can then solve the problem with finite-difference methods. On the boundary and horizon, we will then only evaluate the boundary conditions. The Dirichlet and Robin boundary conditions presented in section 3.1 are finite on those points. Using a high-enough order in the finite difference scheme makes the divergence at δz not too extremely high, not as divergent as required for (adaptive) black-box routines.

The iterative scheme used needs to depart from some ansatz for the solution. It does not necessarily need to be a solution to the equations of motion in some way, but it needs to be 'close enough' to the true solution we are trying to arrive at. The parameters in this scenario are the chemical potential, μ, lattice vector G_x and lattice strength $\mathcal{A}_x$. As I have set the horizon radius $z_h = 1$, the temperature is then set by the chemical potential to be

$$\frac{T}{\bar{\mu}} = \frac{12 - \bar{\mu}^2}{16\pi\bar{\mu}}. \tag{3.17}$$

Convenient as a starting point for the iterative scheme is often to pick the Reissner-Nordström background at the temperature we desire, or otherwise a known numerical solution at parameters close to the ones we desire. Note that in the translationally invariant RN solution, the parameter

G_x does not have any significance.[4] The solutions for small lattice strength $\mathcal{A}_x$ will be close to the analytical Reissner-Nordström solution. The resulting lattices are shown in figure 3.1

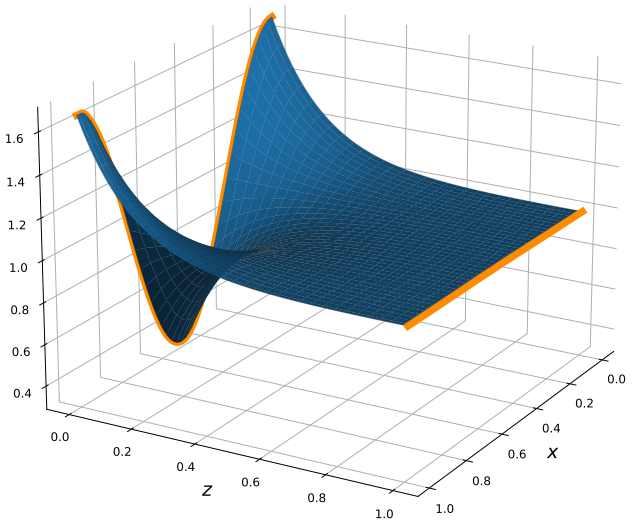

Figure 3.1.: This is an example of a bulk picture of the unidirectional lattice. This particular profile is of the bulk electric field $F_{tz} = -\partial_z A_t$. The parameters here are $T = 0.15\mu$, $G = 4\mu, \mathcal{A}_x = 0.1$.

3.2.1. Numerical Convergence of Holographic Lattices

Testing the validity of an ansatz and the code used to compute the numerical solutions is often one of the most important and yet one of the most easy to overlook parts of writing code. This is especially true in an academic setting, where the desire to get results sometimes outweighs the 'proper' procedure of testing the code thoroughly before using it in production. Furthermore, it can be possible for the code, even if it is not wrong, to give answers that reach unsatisfactory levels of precision at certain parameters. In the holographic lattices, this can for example be caused by low temperatures or large gradients in the problem. Therefore, it is crucial that there are tools available that can be used not only as sanity checks, but also to prove that a given solution to a problem is satisfactory. In this case there are several tools available. The most useful ones are the

[4] This makes for a good check to see if observables are correctly implemented, as the translationally invariant solution should have no mind of any finite G_x whatsoever.

trace of the stress-energy tensor and the DeTurck vector. In the case of the trace of the stress-energy tensor, it is good practice to have the trace vanish to a much greater accuracy than each of its individual components. The DeTurck vector can be shown to be a purely spatial quantity and therefore it is enough to check that its norm $\xi^2 = \xi^\mu \xi_\mu \geqslant 0$ vanishes, rather than having to compute whether each component vanishes independently. In order for precision to be under control, these will need to display some key properties, most importantly that it should show that the knobs we can tune that we expect to increase accuracy actually do so. The unidirectional lattice was the primary inspiration for the Python code, which was written to be a very general n-dimensional (non-)linear PDE solver. As it is written in Python it is not extremely fast, however what it lacks in speed it makes up for in flexibility. It is most suited to two-dimensional differential equations, so that is why the unidirectional lattice together with the radial direction is a good test for its performance. This convergence is shown in figure 3.2. Unsurprisingly, increasing the number of points in the lattice as well as the differentiation order increases the precision. The DeTurck vector shows a similar picture in figure 3.3. The difference between the lowest and higher-order finite difference approximations is large, and the diminishing returns between difference order 6 and higher becomes even more apparent, to the point that beyond 40×80 points there is no benefit to the higher-order differentiations any more.

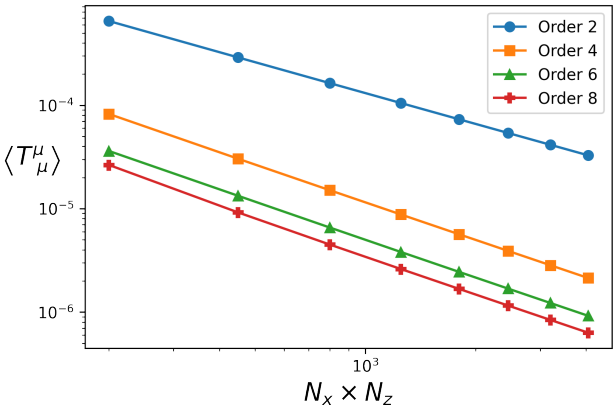

Figure 3.2.: Convergence of the trace of the boundary stress energy tensor as a function of total number of grid points in the problem. For this particular case, the convergence is done at a fixed low temperature and lattice vector as $T = 0.01\mu$, $G = 0.05\mu$, $\mathcal{A}_x = 0.2$, and $N_z = 1.5 \times N_x$. The individual components of T^μ_ν are $O(1)$.

3.2.2. Bidirectional Lattice

The bidirectional lattice has a lot more degrees of freedom to solve for, as there are now N_y times more points in the grid, as well as 15 functions up from 6. In order to tackle this problem, it was necessary to write code in a compiled language. We opted for C, where we were able to use the

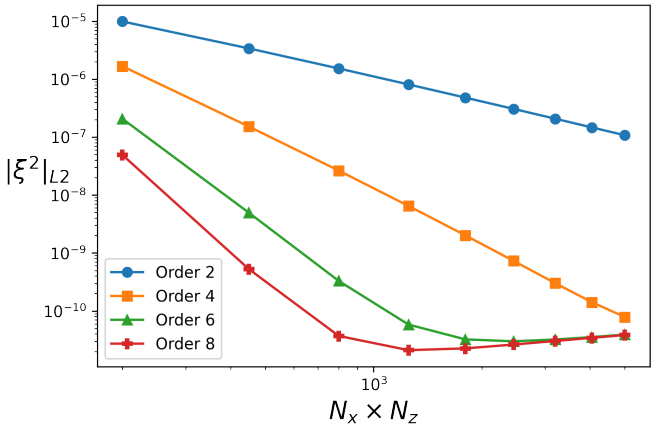

Figure 3.3.: Convergence of the L^2 norm of the ξ^2 over the whole grid. The rate of convergence changes from approximately N^{-1} to N^{-6} when increasing the differentiation order from 2 to 6. Again, this is done at a fixed low temperature and lattice vector as $T = 0.01\mu$, $G = 0.05\mu$, $\mathcal{A}_x = 0.2$, and $N_z = 1.5 \times N_x$.

PETSc library which is suited to run on computing clusters and supercomputers. We can still perform the same convergence checks, however the flexibility of the code is now more limited. In practice, this means that switching differentiation order, which was simply a parameter in the previous code, is now more complicated. The difficulty lies in constructing the Jacobian matrix. This matrix needs to not only couple many fields, but also be consistent in a distributed-memory scheme. While the positions where entries need to be placed is easy to describe an symbolically calculate in a program like Mathematica, this is not easily done in pure C. Therefore, based on the $1D$ results, the order-4 derivatives seem like a good choice. They offer much higher accuracy, but do not increase memory usage by too much, as the number of entries of the matrix per row scales as differentiation order squared due to the mixed derivatives that appear in the expressions. This is clearly seen in figures 3.2 and 3.3. The extra cost in terms of memory use and time it takes to solve makes order 6 and above not worth the trouble.

3.3. Einstein-Maxwell-Dilaton lattices

The Gubser-Rocha black hole that was discussed before in section 2.6 can also be generalised to include translational symmetry breaking effects. The steps that have to be taken to go from the translationally invariant black branes to the EMD lattices is very reminiscent of those necessary to go from the RN black hole to its lattice counterparts.[107] The setup is very similar to the RN ansatz, albeit with one extra field, namely the scalar. In the Gubser-Rocha lattices, we only have access to explicit translational symmetry breaking through the chemical potential, and there are no spontaneous symmetry breaking transitions that we are aware of. The general bidirectional lattice

black hole will have a metric ansatz that looks like

$$\begin{aligned} ds^2 &= \frac{1}{z^2}\left(-Q_{tt}f(z)\eta_t^2 + g(z)\left(Q_{xx}\eta_x^2 + Q_{yy}\eta_y^2\right) + \frac{1}{f(z)}Q_{zz}dz^2\right), \\ \eta_t &= dt \\ \eta_x &= dx + Q_{xy}dy + Q_{xz}dz, \\ \eta_y &= dy + Q_{yz}dz. \end{aligned} \tag{3.18}$$

The gauge field and scalar field will take the form

$$\begin{aligned} A &= A_t dt = \mu\frac{(1-z)}{1+Qz}a_t(x,y,z), \\ \phi &= \frac{\sqrt{3}}{2}\log\left(1+Qz\varphi(x,y,z)\right). \end{aligned} \tag{3.19}$$

The rest of the argument goes much the same way. The boundary conditions are given by an asymptotically AdS boundary and the horizon boundary conditions again arise from a series expansion near the horizon. More tricky, as highlighted in chapter 5, is the boundary condition of the scalar. The boundary condition at $z = 0$ that has been employed here is

$$3Q\varphi + 4\partial_z\varphi - 3Q\varphi^2 = 0 \tag{3.20}$$

which corresponds to an unsourced scalar in mixed $c_\phi = 1/3$ quantisation. This is different from earlier approaches, where the boundary condition do not maintain key properties like conformality of the stress energy tensor in the presence of an explicit lattice.[99]

It will come as no surprise that the derivation of the stress energy tensor and other thermodynamic observables goes in much the same way as the RN black holes the entropy and charge density are easy, as they are given by

$$\begin{aligned} S/\bar{\mu}^2 &= 4\pi\sqrt{(1+Q)^3 Q_{xx}Q_{yy}}/\bar{\mu}^2, \big|_{z=1}, \\ \rho/\bar{\mu}^2 &= \left((1+Q)a_t - \partial_z a_t\right)/\bar{\mu}\big|_{z=0}. \end{aligned} \tag{3.21}$$

The stress tensor now acquires components not only from the third derivative of the metric fields, but also from the source and VEV of the scalar field through the ϕ-dependent terms in equation (2.71). The full expressions are too long to be included here, but the general structure follows that of table 3.1. Using the near-boundary expansions we can deduce that the trace of this does indeed vanish, giving us always conformal matter, as in the homogeneous case.

3.4. Computing Perturbations

Thermodynamics of the black hole states are good first observables, as they can readily be evaluated from black hole backgrounds by simply reading off certain components. As mentioned before, it is quantities like (thermo)electrical conductivities that we really would like to be able to work with.

In general, many of the quantities that are relevant to physical experiment, such as momentum susceptibilities, conductivities, viscosities and much more can be expressed in terms of two-point functions in the field theory. The procedure to do this is fairly standard, but nonetheless requires a great deal of numerical effort in order to extract worthwhile information at physically interesting parameters. The principle is again the same as in section 2.4.2. Some of the components of the metric and gauge field are perturbed without back-reaction. The equations of motion are then expanded to linear order which gives access to two-point functions in the field theory. The difficulty comes mainly because of the nature of the problem. Not only are the fields at finite frequency and momentum complex-valued, which generally restricts the number of useful numerical solvers and preconditioning routines that exist for the problem[5], but the problem is also a linear rather than non-linear one. While this removes the need to make many solutions and updates, it does mean that to get a good solution the differential equation we need to solve with higher accuracy, as we cannot rely on the guarantee that if we make a 'good enough' update step we still get to a good solution as is the case in the non-linear case. Instead, we need to make sure that we get the solution correct directly. This is in general a tricky thing, and here I present only the overview to show how these techniques are all connected. Many of the results in this section only make sense in the context of a particular lattice setup but the methods will carry over onto other setups too.

3.4.1. Optical Conductivities in the Homogeneous Reissner-Nordström Black Hole

The translationally invariant RN black hole forms a good starting point for these considerations. The quintessential example is the electrical conductivity, which is why it featured prominently for pure AdS in section 2.4.2. What is new here is that at finite chemical potential, there are multiple modes that start to couple in to the electrical conductivity. In particular, if we perturb the gauge field by

$$A_x = \delta A_x(z) e^{-i\omega t} \tag{3.22}$$

we can see that this couples to metric perturbations

$$g_{xt} = \delta h_{xt}(z) e^{-i\omega t}, \quad g_{xz}(z) = \delta h_{xz}(z) e^{-i\omega t}. \tag{3.23}$$

There is a lucky coincidence here as it is possible to make a gauge choice to be in radial gauge to make h_{xz} vanish, and by combining the other two equations of motion the problem can be reduced to a single second order ordinary differential equation for $A_x(z)$. The resulting equation in terms of the chemical potential μ, the emblackening factor $f(z)$ and the parameter γ as [132]

$$(f\delta A_x')' + \frac{\omega^2}{f}\delta A_x - \frac{4\mu^2 z^2}{\gamma^2}\delta A_x = 0. \tag{3.24}$$

This equation does not have a simple analytical solution, and is only able to be solved numerically. Boundary conditions come from sourcing the (perturbative) electric field $f_{tx} = \partial_t A_x$ along with

[5] It is possible to phrase the problem in terms of coupling of real fields by expanding the real and imaginary parts separately, but that doubles the number of fields and equations in the problem which severely hinders performance.

insisting on computing the retarded Green's function, as this is the physically most relevant one. If we take out an oscillating factor

$$A_x(z) = f(z)^{-4\pi i\omega/T}\tilde{A}_x(z), \tag{3.25}$$

then infalling boundary conditions can be imposed by requiring $\tilde{A}_x$ to be a series expansion in $(z-1)$. This gives us the retarded Green's function. In general setups, this then gives the same kind of boundary condition expansions as in the lattice, where we can fix the first-order expansion coefficient at the horizon in terms of the horizon values. The conductivity is given by

$$\sigma(\omega) = \left.\frac{A_x'}{i\omega A_x}\right|_{z=0}. \tag{3.26}$$

Since the equation is linear, we can then fix the boundary condition at the boundary to simply be $A_x(z=0)=1$, as we only fix the ratio of coefficients in the expansion at the horizon, and not the value itself.[6] Equation (3.26) then takes care that only the ratio of subleading to leading component is read off, not the actual value of the solution which is rather arbitrary.

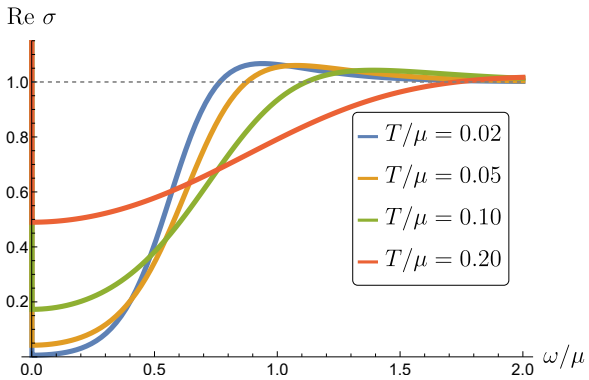

Figure 3.4.: AC conductivity of the RN black hole at finite frequency for different temperatures. Notice how in the high-frequency limit $\omega \gtrsim \mu$, the optical conductivity approaches the zero-density CFT limit $\sigma(\omega) = 1$.

The resulting conductivity can be seen at different temperatures in figure 3.4. Spectral weight is transferred from $\omega < 1$ to $\omega \gtrsim 1$ when temperature is lowered, and a depletion of the conductivity appears to happen for low frequency. The intensity of this depletion increases for lower temperature. Note that the $\omega = 0$ value is divergent due to translational symmetry of the solution. This can also be checked in Kramers-Kroning consistency, which indeed produces a $1/\omega$

[6] There are many other methods of computing conductivities, such as shooting methods and other bulk matching procedures. However, since we have access to a general way of computing partial differential equations through the solver I have developed, it is much more convenient to phrase this in the same framework as the earlier backgrounds and the lattice conductivities as well.

behaviour for $\omega \to 0$.[133, 134] This kind of result can actually be seen in real condensed matter systems, for example in graphene, which also has a dip below $\omega = \mu$ but recovers a constant $\sigma(\omega) = 1$ at high frequency, as expected for a $2+1$ dimensional CFT.

3.4.2. Finite Momentum Correlators

Of course, there is more to transport than just computing the electrical conductivity. Maintaining the fluid analogy, the current-current correlator should be governed by several poles, for example a sound mode in the longitudinal sector and a shear mode in the transverse sector. However, it is not possible to identify these in the homogeneous model unless we go to finite momentum of the correlator, as we require the vector momentum in order to define transverse and longitudinal directions. At $k = 0$, only modes in the spin zero-sector can appear. The general ansatz for the pertubation at finite frequency and momentum is

$$\begin{aligned} g_{\mu\nu} &= g^{(0)}_{\mu\nu} + \varepsilon h_{\mu\nu}(z) e^{-i(\omega t - k_x x - k_y y)} + O(\varepsilon)^2, \\ A_\mu &= A^{(0)}_\mu + \varepsilon b_\mu(z) e^{-i(\omega t - k_x x - k_y y)} + O(\varepsilon)^2. \end{aligned} \tag{3.27}$$

$g^{(0)}$ and $A^{(0)}$ are the background values of the metric and gauge field that have already been computed. If we enter this ansatz into the equation of motions (3.2), at first order in ε we will get a linear set of coupled differential equations for the perturbations in the presence of a fixed background. Using the translationally invariant Reissner-Nordström background, the perturbations will not in general have any more dependence on the transverse directions x, y other than in the oscillating exponential. As the background is rotationally invariant, we can freely pick $\vec{k} = k\hat{x}, k_y = 0$. In this case now, the modes $h_{ty}, h_{xy}, h_{zy}, b_y$ are odd under parity $y \to -y$ and will therefore decouple from the rest of the perturbations which are even under parity. The even-parity modes will be the fields that couple in the longitudinal sector, and the odd-parity modes correspond to transverse sector.[135] There is a rather large amount of gauge freedom left in the equations at the moment, stemming from diffeomorphism invariance and $U(1)$ gauge symmetry of the Maxwell field. Common choices to fix the gauge are the radial gauge, which simply sets [135]

$$h_{\mu z} = b_z = 0. \tag{3.28}$$

Another popular gauge choice is DeDonder and Lorenz gauges, where [136]

$$\nabla^\mu \left(\bar{h}_{\mu\nu} = 0 \right), \quad \nabla^\mu b_\mu = 0, \tag{3.29}$$

where $\bar{h}$ is the trace-reversed perturbation metric

$$\bar{h}_{\mu\nu} = h_{\mu\nu} - \frac{1}{2} \mathrm{Tr}(h) g^{(0)}_{\mu\nu}. \tag{3.30}$$

This is in principle a general ansatz for computing any perturbation we wish. When sourcing the correct components of $h_{\mu\nu}$, one can for example compute correlators

$$G_{T^{\mu\nu}T^{\mu\nu}}(\omega, k) \sim \left\langle h_{\mu\nu} h_{\mu\nu} \right\rangle. \tag{3.31}$$

In the case of the homogeneous RN black hole things simplify tremendously, and it is possible to make some clever combination of fields into what are called the master field equations.[135, 137, 138] This however is rather specific and does not apply whenever a lattice is in play. Therefore, I will not expand in great detail on this procedure in here. Instead, let us stay focused on electrical conductivity. The choice of transverse or longitudinal sector will come from our choice of electric field. The source of the electric field turns out to be the value of the $b_{x,y}$ perturbations at the boundary

$$E_x = f_{tx}\big|_{z=0}, \qquad E_y = f_{ty}\big|_{z=0} \tag{3.32}$$

while the responses are

$$J_x = f_{zx}\big|_{z=0}, \qquad J_y = f_{zy}\big|_{z=0} \tag{3.33}$$

where $f_{\mu\nu}$ is the field strength tensor at first order in the perturbation parameter ε. This corresponds to picking

$$E_x = i\omega b_x(z=0), \qquad E_y = i\omega b_y(z=0). \tag{3.34}$$

For the electrical conductivity, the correlators are computed

$$G_{J^iJ^j}(\omega,k) = \left.\frac{\partial_z b^i(\omega,k,z)}{b_j(\omega,k,z)}\right|_{z=0}. \tag{3.35}$$

The conductivity then we need to keep in mind that at finite momentum, we need to subtract the real part of the zero-frequency limit of the correlator in order to remove certain contact-like terms [81, 139]

$$\sigma(\omega,k) = \frac{G(\omega,k) - \operatorname{Re} G(\omega,k\to 0)}{i\omega}. \tag{3.36}$$

In the translationally invariant situation, we expect two things depending on the direction of k with respect to E. In the longitudinal channel, where $\vec{k} \parallel \vec{E}$, we expect to see a sound-like response, with a corresponding sound peak at some $\omega = v_s k$ where v_s is the sound velocity. This kind of response is shown in figure 3.5a. There is also a diffusion pole which causes some momentum dissipation near $\omega = 0$, but in the specific case of longitudinal conductivity this is suppressed by a factor ω^2/k^2. In the transverse case, where $\vec{k} \perp \vec{E}$, we expect to see a diffusion pole appear. At low $\vec{k}/\mu$ this will form a weak source of momentum relaxation. As a result, we expect a small Drude peak to form in the low-frequency regime. This is shown in figure 3.5b.

3.4.3. Lattice Conductivities

In the presence of a lattice, either uni- or bidirectional, this story changes in essence very little. Again we can write the perturbations similar to equation (3.27), but now with the added modification that the perturbations also acquire a spatial modulation

$$\begin{aligned} h_{\mu\nu}(z)e^{-i\left(\omega t-\vec{k}\cdot\vec{x}\right)} &\to h_{\mu\nu}(x,y,z)e^{-i\left(\omega t-\vec{k}\cdot\vec{x}\right)}, \\ b_{\mu}(z)e^{-i\left(\omega t-\vec{k}\cdot\vec{x}\right)} &\to b_{\mu}(x,y,z)e^{-i\left(\omega t-\vec{k}\cdot\vec{x}\right)}. \end{aligned} \tag{3.37}$$

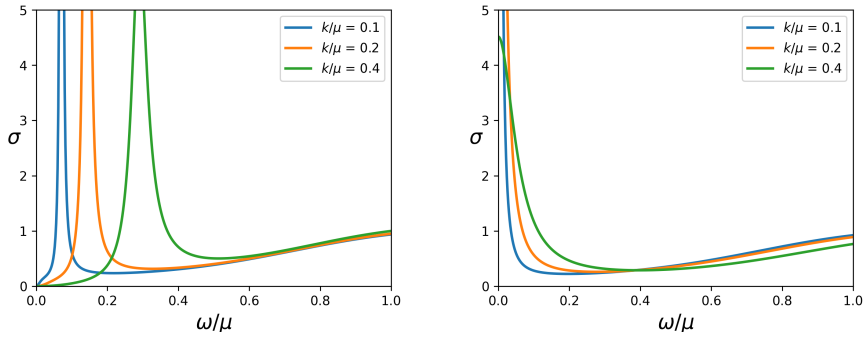

(a) Longitudinal optical conductivity. For larger values of k, the sound peak moves to higher frequency and broadens, indicating increased attenuation.

(b) Transverse optical conductivity. Note that for higher k, the Drude peak lowers and becomes wider.

Figure 3.5.: Optical conductivity at finite momentum in RN. We choose here a constant source E_x, and let $\vec{k} = k\hat{x}$ or $\vec{k} = k\hat{y}$ for longitudinal and transverse computations, respectively. In both cases, for large ω the CFT result $\sigma(\omega) \to 1$ is recovered.

The difference now is that the exponentials are not a periodic function on the domains L_x, L_y, while the perturbations are assumed to be. This is reminiscent of a Bloch wave expansion for perturbations that is common in condensed matter physics. The principle of solving the equations is still a relatively simple affair, as the principle is the same as in all the cases before. The main difference is that now this turns into a set of linear partial differential equations rather than a set of linear ordinary ones. The horizon boundary conditions are also given by requiring an order-by-order solution of the equations of motion near the horizon to the infalling waves. The argument that from symmetry k_y can be set to zero in general is lost, because the uni- and bidirectional lattices break rotational invariance badly. Another difference is that now the differential equation for the perturbations has to be computed on a given (numerical) background. The variable coefficients in the differential equations are then also dependent on a set of background fields instead of just the radial coordinate. The gauge fixing terms described in section 3.4.2 still apply, and will now in general depend on both spatial dimensions as well as background fields. This is mainly a practical challenge from a programming point of view, not from a conceptual one. The evaluation of the correlator is then the same as in equation (3.35), with the added point that we need to average over the spatial dimensions in order to get the proper response.[7] The optical responses in several types of 1D holographic lattices have been extensively studied in other works.[107, 118, 120, 136, 140] The main result that can be highlighted here is that in the presence of a weak (ionic or other) lattice, there is also a small amount of momentum relaxation, as in the case of the transverse conductivity

[7] Since we always take the source to be spatially homogeneous, the average only needs to be done over the expectation value. It is possible to do both finite wave vector sourcing and responses, see the discussion on inverting the alternate quantization later in chapter 4.

in pure RN, but now also in the $k = 0$ channel. As a result, we again expect a finite Drude peak to appear.

3.4.4. DC conductivities

The limit $\omega \to 0$ in the definition of the conductivity as in equation (3.36) is problematic when we try to deal with conductivity at zero-frequency. Namely, the DC limit is well defined, but evaluating at exactly $\omega = 0$ contains a divide-by-zero, which is something that computers do not handle well. DC transport contains a lot of information about the system and therefore it is good to have access to it. Conveniently, there is an easier way to find these. In general, they are computed by taking particular combinations of time-independent perturbations to the metric and gauge field. This procedure has been investigated in great detail, with an interesting result at the end. It turns out that the DC conductivity in both Reissner-Nordström and dilatonic black holes can be evaluated by solving a Stokes flow-like problem at the black hole horizon.[114, 140–146]

In the most general setting, where we not only have the Einstein-Maxwell action but potentially also other scalar fields, it turns out that by perturbing the black hole just right and using the symmetries in the equation of motion the horizon equations that need to be solved becomes a system of four equations, where [142, 146]

$$\begin{aligned} &\eta_H \left(-2\nabla^j \nabla_{(i} v_{j)} + v^j \nabla_j \phi^{(h)} \nabla_i \phi^{(h)}\right) - d\chi^{(h)}_{ij} Q^j - F^{(h)}_{ij} J^j - \\ &\rho_H \left(E_i + \nabla_i w\right) - T s_H \left(\zeta_i - \nabla_i \frac{p}{4\pi T}\right) = 0, \\ &\partial_j Q^j = 0, \qquad \partial_j J^j = 0. \end{aligned} \tag{3.38}$$

These η_H, s_H, ρ_H are horizon quantities that play the role of shear viscosity, entropy and charge density in this Stokes-like problem for a fluid with velocity v_j, pressure p and forcing term w_j living on the black hole horizon. s_H is the same as the entropy we assign to the black hole when considering its thermodynamics, and $\eta_H \equiv s_H/4\pi$, akin to the famous result for minimal viscosity.[85] Additionally, one can find that $\nabla_j v^j = 0$ must also be satisfied, making this a Stokes-flow like incompressible flow problem. The thermal and electrical gradients are here sourced by ζ_i, E_i and can in principle depend on spatial position, although I will not consider that in this thesis. The unknowns here are the field v^j, w, p, while the rest of the quantities are given in terms of bulk fields evaluated at the horizon. Q_i, J_i are the resulting heat and electrical currents. These are defined on the horizon, but it can be shown that their unit cell averages $\bar{Q}, \bar{J}$ are not renormalised from the horizon to the boundary, and are therefore equal to the averages of the DC currents we want to interpret in the boundary theory. The conductivities are then found with

$$\begin{pmatrix} \bar{J}^i \\ \bar{Q}^i \end{pmatrix} = \begin{pmatrix} \sigma^{ij} & T\alpha^{ij} \\ T\bar{\alpha}^{ij} & T\bar{\kappa}^{ij} \end{pmatrix} \begin{pmatrix} E_j \\ \zeta_j \end{pmatrix}. \tag{3.39}$$

Here $\alpha, \bar{\alpha}$ are the thermoelectric conductivities and $\bar{\kappa}$ is the thermal conductivity.

The exact forms of these depend on the exact setup that is being used.[142] What is the case is that this simplifies in certain scenarios. Specifically, if translational symmetry is broken in some

kind of homogeneous way, where there is no lattice, the thermoelectric conductivity can be evaluated by just evaluating certain horizon quantities. The case of the unidirectional lattice is simple too, where now thermoelectric currents can be expressed in terms of integrals over horizon quantities.[140] For the bidirectional lattice due to the lack of remaining symmetries there is no such simplification and one has to resort to actually solving the Stokes differential equations (3.38) numerically. This can be done rather simply, as this is just yet another modification of the code solving a perturbative problem in the presence of a background, like in the AC case, but now restricted to only the horizon.[8]

3.5. Outlook

All this together provides a lightning overview of the methods that have been used in the production of this thesis. The results of these endeavours will be presented in the following chapters, in papers on fermionic spectral functions in holographic lattices, optical and DC conductivities in Gubser-Rocha black holes, and thermodynamics and quantization considerations in the Gubser-Rocha model. All the numerics contained therein are based on the equations that have been presented here. Their practical efficient implementation into computer code is a story in and upon itself, which unfortunately could not be included in this thesis due to constraints of length. For this in-depth discussion on the numerical solutions of non-linear elliptic boundary value problems in two and three dimensions, there are more in-depth discussions available.[147]

[8] One thing to keep in mind for accuracy is that in the way the setup is currently phrased, there are zero modes present for the fields p, w, as they can be augmented by a constant shift $p \to p + c$, without changing the Stokes equations, as they only appear as derivatives in the Stokes equations. In order to get a correct linear solve, one should expect to have to fix the values of p, w at some point in the domain. This will remove the zero (or often numerically very small) pair of eigenvalues from the matrix that is used to solve the problem.